Supporting Information for

Energy Efficient Artificial Synapses Based on Oxide Tunnel Junctions

Jiankun Li,[†] Chen Ge,[*,†,‡] Haotian Lu,[§] Haizhong Guo,[‖] Er-Jia Guo,[†,⊥] Meng He,[†] Can Wang,[†,‡,#] Guozhen Yang,[†] Kuijuan Jin[†,‡,#]

[†]Beijing National Laboratory for Condensed Matter Physics, Institute of Physics, Chinese Academy of Sciences, Beijing 100190, China

[‡]School of Physical Sciences, University of Chinese Academy of Science, Beijing 100049, China

[§]Department of Electrical and Computer Engineering, University of Illinois, Urbana-Champaign, 61820, Illinois, USA

[‖]School of Physical Engineering, Zhengzhou University, Zhengzhou, Henan 450001, China

[⊥]Center of Materials Science and Optoelectronics Engineering, University of Chinese Academy of Sciences, Beijing 100049, China

[#]Songshan Lake Materials Laboratory, Dongguan, Guangdong 523808, China

*Corresponding Author.

E-mail address: gechen@iphy.ac.cn

KEYWORDS: artificial synapses, oxide tunnel junction, synaptic plasticity, oxygen vacancy, pulsed laser deposition

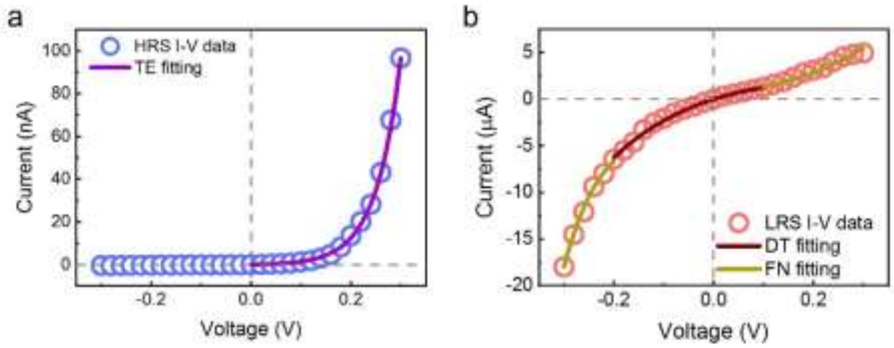

Figure S1. Representative *I-V* curves at HRS and LRS. a) Measured (open circles) and fitted (line) *I-V* curves of HRS. b) Measured (open circles) and fitted (line) *I-V* curves of LRS.

Note S1.

At HRS, thermionic emission (TE) currents under forward bias ($V > 3k_BT/q$) across the Schottky could be written as[1]

$$I = SA^*T^2\theta_n \exp(-\frac{\Phi_B}{k_BT})\exp(\frac{qV}{nk_BT}) \tag{1}$$

where A* is the standard Richardson constant, Φ_B is the Schottky barrier height, T is the absolute temperature, k_B is the Boltzmann constant and n is the ideality factor. In the calculations, A*=156 A cm^{-2} K^{-2}. Through fitting the *I-V* curve at HRS, the calculated Schottky barrier height is about 0.55 eV.

At LRS, direct tunneling (DT) is conspicuous at a low voltage and Fowler-Nordheim tunneling (FNT) dominates at a high voltage. The DT current through a trapezoidal barrier can be described as[2]

$$I_{DC} = -S\frac{4em^*}{9\pi^2\hbar^3}\frac{\exp\{\alpha(V)[(\Phi_2-\frac{eV}{2})^{\frac{3}{2}}-(\Phi_1+\frac{eV}{2})^{\frac{3}{2}}]\}}{\alpha^2[(\Phi_2-\frac{eV}{2})^{\frac{1}{2}}-(\Phi_1+\frac{eV}{2})^{\frac{1}{2}}]^2}\times\sinh\{\frac{3}{2}\alpha(V)[(\Phi_2-\frac{eV}{2})^{\frac{1}{2}}-(\Phi_1+\frac{eV}{2})^{\frac{1}{2}}]\frac{eV}{2}\} \tag{2}$$

where $\alpha = \frac{4d(2m^*)^{\frac{1}{2}}}{3\hbar(\Phi_1+eV-\Phi_2)}$, Φ_1 and Φ_2 are the barrier height at Pt/STO and STO/SNTO interface, respectively. S is the junction area, m* is the effective electron mass, ħ is the reduced Planck constant and d is the STO barrier width of about 2.8 nm. Here, Φ_1 and Φ_2 are used as fit parameters to describe the direct tunnelling through a trapezoidal potential barrier. The calculated Φ_1 and Φ_2 are 0.35 eV and 0.41 eV for STO based tunnel junctions.

The Fowler-Nordheim (FN) tunneling corresponds to electrodes tunneling across a triangular-shaped potential barrier, when an electrical field E is applied to a rectangular or trapezoidal barrier. The current is given by[3]

$$I_{FN} = S\frac{e^3}{8\pi h\Phi_i}(\frac{V}{d})^2\exp[-\frac{8\pi\sqrt{2m^*}d\Phi_i^{\frac{3}{2}}}{3heV}] \tag{3}$$

where Φ_i is the height of trapezoidal barrier. In our experiment, we estimate that the threshold voltages for transition from DT to FNT are -0.2 V and +0.1 V, respectively. According to the fitting results of the FNT model, Φ_i was found to be 0.075 eV.

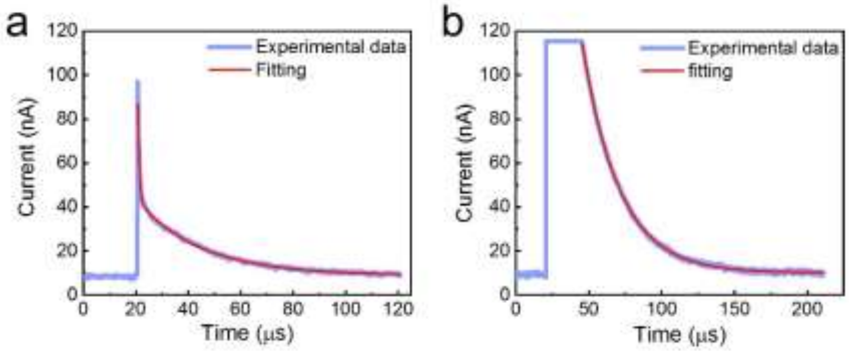

Figure S2. Exponential fitting of the decay curves of short term memory (STM). The current-time (*I-t*) curves are triggered by pulses with a duration of 50 ns, amplitudes of 1 V (a) and 1.2 V (b) with a compliance of 115 nA. The relaxation time constant τ_1 are 23.5 μs for (a) and 25.4 μs for (b), respectively.

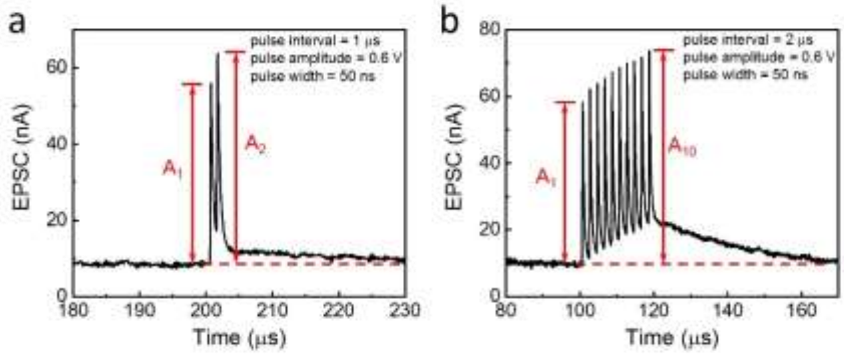

Figure S3. The paired-pulse facilitation (PPF) and PTP behavior of the OTJs. (a) The EPSC curve triggered by double spikes. A_1 and A_2 are the peak values of the first and second spikes. (b) The EPSC curve triggered by ten spikes. A_{10} is the peak value of the tenth spike. The background bias is 0.1 V.

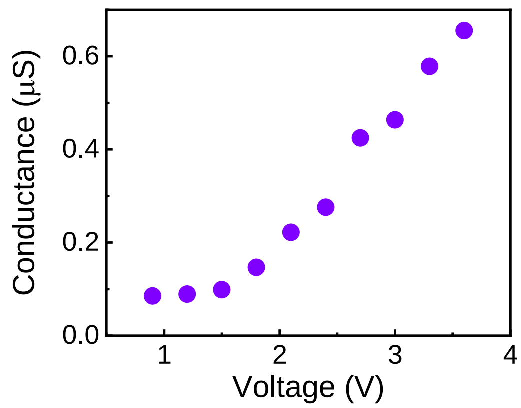

Figure S4. The conductance variation after the pre-synaptic spikes.

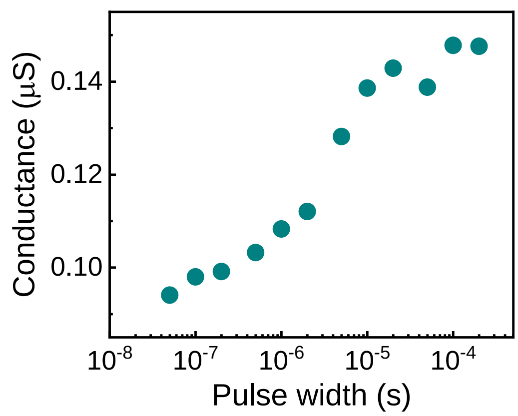

Figure S5. The conductance variation after pre-synaptic spikes with different durations.

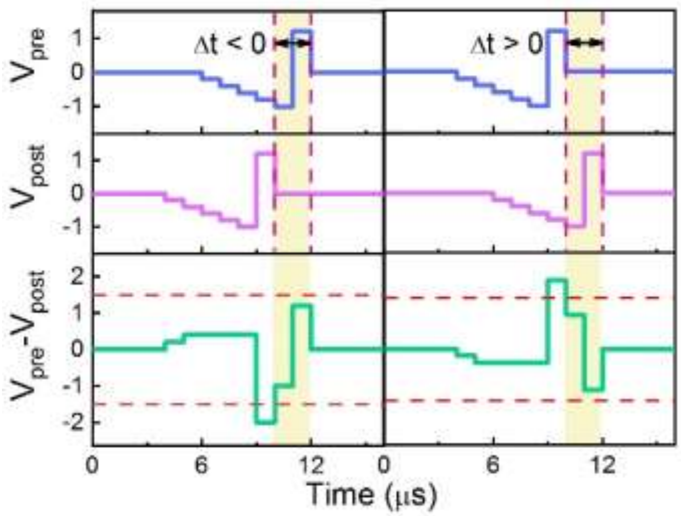

Figure S6. Sketch of the antisymmetric STDP learning shape. The voltage of pre- and post-synaptic spike and their sum are represented by V_{pre}, V_{post} and V_{pre}-V_{post}, respectively. The red horizontal lines are the threshold voltages of ± 1.5 V.

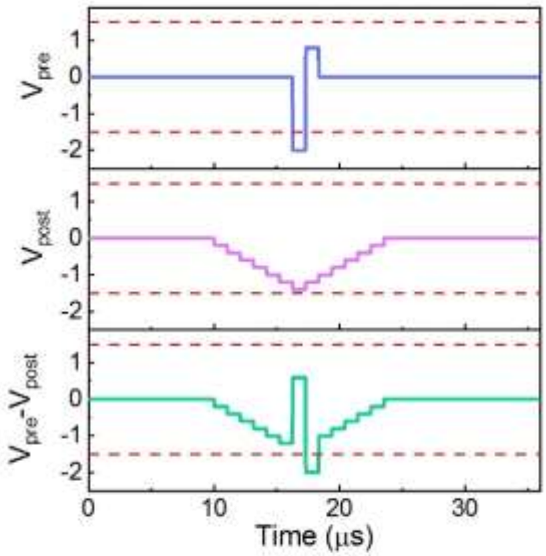

Figure S7. Sketch of the symmetric STDP learning shape. The voltage of pre- and post-synaptic spike and their sum are represented by V_{pre}, V_{post} and V_{pre}-V_{post}, respectively. The red horizontal lines are the threshold voltages ($\pm$1.5 V).

REFERENCE

(1) Mikheev, E.; Hoskins, B. D.; Strukov, D. B.; Stemmer, S. Resistive Switching and its Suppression in Pt/Nb:$SrTiO_3$ Junctions. *Nat. Commun.* **2014**, *5*, 3990.

(2) Hu, W. J.; Wang, Z.; Yu, W.; Wu, T. Optically Controlled Electroresistance and Electrically Controlled Photovoltage in Ferroelectric Tunnel Junctions. *Nat. Commun.* **2016**, *7*, 10808.

(3) Rana, A.; Lu, H.; Bogle, K.; Zhang, Q.; Vasudevan, R.; Rhakare, V.; Gruverman, A.; Ogale, S.; Valanoor, N. Scaling Behavior of Resistive Switching in Epitaxial Bismuth Ferrite Heterostructures. *Adv. Funct. Mater.* **2014**, *24*, 3962.